Cement and Concrete Research 41 (2011) 842–846

Contents lists available at ScienceDirect

Cement and Concrete Research

journal homepage: http://ees.elsevier.com/CEMCON/default.asp

Influence of nucleation seeding on the hydration kinetics and compressive strength of alkali activated slag paste

Mija H. Hubler [a], Jeffrey J. Thomas [b,*], Hamlin M. Jennings [c]

[a] Dept. of Civil and Environmental Engineering, Northwestern University, Evanston, IL 60208, USA
[b] Schlumberger-Doll Research, Cambridge, MA 02190, USA
[c] CSHub, Dept. of Civil and Environmental Engineering, MIT, Cambridge, MA 02190, USA

ARTICLE INFO

Article history:
Received 21 December 2010
Accepted 1 April 2011

Keywords:
Kinetics (A)
Compressive strength (C)
Alkali activated cement (D)
Granulated blast-furnace slag (D)

ABSTRACT

Addition of pure calcium silicate hydrate (C–S–H) to alkali-activated slag (AAS) paste resulted in an earlier and larger hydration rate peak measured with isothermal calorimetry and a much higher compressive strength after 1 d of curing. This is attributed to a nucleation seeding effect, as was previously established for Portland cement and tricalcium silicate pastes. The acceleration of AAS hydration by seeding indicates that the early hydration rate is controlled by nucleation and growth. For the experiments reported here, the effect of C–S–H seed on the strength development of AAS paste between 1 d and 14 d of curing depended strongly on the curing method. With sealed curing the strength continued to increase, but with underwater curing the strength decreased due to cracking. This cracking is attributed to differential stresses arising from chemical and autogenous shrinkage. Similar experiments were also performed on Portland cement paste.

1. Introduction

Blast furnace slag is an industrial byproduct that has been used effectively as a partial replacement for Portland cement to improve the long term properties of concrete and to reduce the carbon footprint associated with cement manufacture [1–3]. Slag is a latent hydraulic material, meaning that it has little hydraulic activity when mixed with pure water, but becomes activated by the high pH of the cement pore solution so that it reacts along with the cement, forming similar hydration products. This activation is due to the increase in the solubility, and thus the dissolution rate, of glassy phases in the slag with higher pH [3,4]. The durability of concrete made with various blends of slag and cement has been monitored over periods of up to 40 years and found to be excellent [5]. Another approach is to activate pure slag by using chemicals such as sodium hydroxide, sodium silicate, or calcium carbonate to increase the pH [6,7]. Such alkali-activated slag (AAS) cement and concrete are even more desirable from an environmental standpoint, and can have beneficial properties such as high strength.

The hydration of slag forms calcium silicate hydrate (C–S–H) as its primary hydration product, as with Portland cement. However, in the case of slag the Ca/Si molar ratio is much lower, generally close to 1, and the degree of aluminum substitution is higher. The morphology of the hydration products is also different. AAS paste has a higher proportion of mesopores in the size range of a few nm, which create large shrinkage stresses when they empty [3,8–13]. At the same time, AAS paste has less capillary pore volume than Portland cement paste made at the same water/cement ratio, leading to a lower permeability, particularly at early ages. Drawbacks to the use of AAS concrete include a greater amount of autogenous and drying shrinkage [9,12–14], susceptibility to cracking [8,9,15] and the cost of the activator [2,7,10,12]. A better understanding of the hydration mechanisms of blast-furnace slag is needed to develop new methods of activation and to optimize its properties.

Recently, it was shown that the addition of pure, laboratory-synthesized C–S–H accelerates the hydration of C_3S and Portland cement by seeding the hydration process, providing additional nucleation sites for the growth of hydration product [16]. Seeding with C–S–H is a useful way to investigate the early hydration mechanisms because the accelerating properties of the C–S–H seed rely on nucleation and growth being the rate limiting step in the hydration process. The presence of C–S–H has little or no effect on the composition of the pore solution, so if the rate-limiting step is the rate of dissolution of the cementitious component, then the seed should have little or no effect on the kinetics. However, if the reaction is nucleation and growth limited, then the seeding effect of the C–S–H will result in significant acceleration, as previously observed.

In the present study, the effects of C–S–H seed on the hydration kinetics and compressive strength development of AAS paste and OPC paste were investigated. For pure (non-activated) slag, the C–S–H seed has little effect, indicating that the rate of dissolution of the slag is rate controlling. However, when the slag is activated with sodium silicate (AAS), then the addition of C–S–H has an accelerating effect, significantly shortening the time to reach the early hydration rate peak. This provides the first unambiguous evidence that the AAS hydration process occurs by nucleation and growth, as is the case with C_3S and Portland cement.

---

* Corresponding author.
E-mail address: jthomas39@slb.com (J.J. Thomas).

doi:10.1016/j.cemconres.2011.04.002

The effects of C–S–H on the compressive strength of AAS paste and OPC paste were complex. For OPC paste, seeding increases the compressive strength at 1 d and 3 d, but at ages between 7 d and 28 d the strengths of seeded and unseeded pastes are similar. For AAS paste, the effects of seeding on strength depend strongly on the method of curing. With sealed curing conditions, the addition of seed significantly increases the compressive strength at all ages between 1 and 14 d. However, when cured underwater, the strength of a seeded paste is lower than that of an unseeded AAS paste at ages greater than 1 d. A hypothesis related to the development of an internal stress gradient and associated cracking is advanced to explain this behavior.

2. Experimental section

A commercial ground slag product (NewCem, Lafarge) was used in this study. The alkali activator was solid sodium metasilicate ($Na_2SiO_3 \cdot 5H_2O$), which was added in amounts ranging from 0 to 10 mass% by mass of slag. The OPC specimens were made with Type I OPC cement (Lafarge).

The C–S–H seed was formed as described previously [16]. Separate solutions of sodium metasilicate ($Na_2SiO_3 \cdot 5H_2O$) and calcium nitrate ($Ca(NO_3) \cdot 4H_2O$) in deionized water were prepared such that the molar ratio of CaO to SiO_2 would be 1. The solutions were then combined, causing C–S–H to precipitate. The precipitated solution was shaken for 15 min and then filtered using a Buchner funnel while rinsing with a CaO solution to remove adsorbed sodium and nitrate ions from the C–S–H. The concentration of CaO in the rinse solution was selected to match the solubility of the precipitated C–S–H. After filtering, the resulting C–S–H gel was stored in a sealed container. For each batch of C–S–H created, the mass fraction of solid C–S–H was determined by measuring the weight loss of a small sample of the gel after drying at 160 °C for 12 h. The mass fraction of solids in the C–S–H seed batches was 5.2 ± 0.4%. This measure of solid C–S–H likely includes a small amount of chemically combined water.

C–S–H seed was added to the pastes at a predetermined mass percentage of solid C–S–H by mass of slag or cement. The water associated with the C–S–H seed was accounted for in calculating the water to binder ratio (w/b). To ensure an even distribution of seed within the paste, the seed was first blended with the remaining mix water for 5 min using a handheld shear mixer. The resulting fluid exhibited strong shear thickening behavior that persisted when mixed with the sodium silicate and dry slag. This procedure eliminated the appearance of pockets of unmixed seed in the interior of the specimens, which were otherwise visible when inspecting the fragments following a compressive strength test.

To mix the AAS pastes, the slag and sodium silicate activator were first dry mixed and then stirred into the preblended seed/water mixture and mixed by hand for up to 10 min. These pastes were very thick and difficult to mix initially, but attained a fluid consistency after several minutes of vigorous hand mixing. Preliminary experiments were also conducted using a commercial paddle mixer, but these pastes formed large internal voids and had lower compressive strengths, so this procedure was discontinued. The addition of superplasticizers is known to improve the workability of AAS pastes [17], but was avoided in this study to eliminate the potential effects on the kinetics and strength, and simplify the interpretation.

To determine the effect of seeding on the compressive strength, it was necessary to compare seeded and unseeded pastes at the same w/b. Unseeded AAS paste was found to bleed at w/b values above 0.43, giving an upper limit of w/b. In order for a seeded AAS paste to be workable at w/b = 0.40, the maximum seed addition was 1%. At w/b = 0.43, the maximum seed addition was 1.5%. A workable paste was expected to flow on its own or when vibrated locally.

An isothermal calorimeter (Model 4200, Calorimetry Sciences Corporation, Linden, UT) was used to study the early hydration kinetics of the slag pastes. The calorimeter was set to 20 °C with a time resolution of 1 min. Immediately after mixing, approximately 1 g of paste was sealed in a 1.3 mL glass ampule and placed into the instrument.

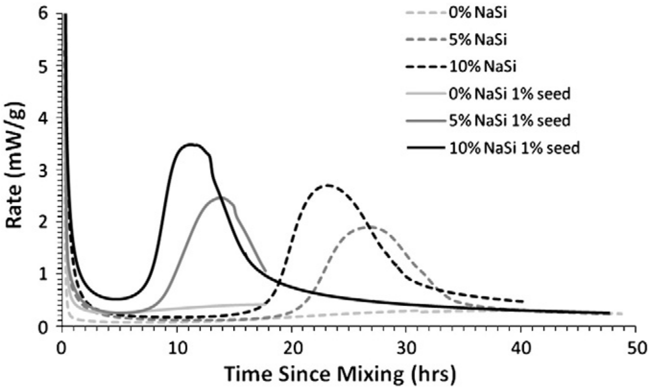

Fig. 1. Rate of heat evolution at 20 °C of slag pastes activated with 0%, 5%, or 10% sodium metasilicate and made with 1% C–S–H seed (solid lines) or without seed (dotted lines). All pastes were made with w/b = 0.40.

Compressive strength tests were performed on standard compression cylinders 2 in diameter by 4 in height. The plastic molds were filled with mixed paste in three lifts. These specimens were cured at room temperature in either underwater or sealed conditions. For underwater curing, the specimens were stored in a curing room with 100% humidity during the first 24 h. They were then demolded and cured under lime water until tested. For sealed curing the pastes remained sealed inside the plastic molds until shortly before the test.

Compression tests were performed using a Brainard-Kilman displacement driven concrete compression machine after curing times ranging from 1 d to 28 d. For each age and paste type, three specimens were tested and the results were averaged.

3. Results

3.1. Hydration kinetics

Fig. 1 shows the effect of 1% C–S–H seed addition on slag pastes made with 0%, 5%, or 10% sodium metasilicate activator. The paste without seed or activator (i.e., pure slag) has very low heat output, as expected. The addition of 5% or 10% activator in the absence of seed causes a well-defined hydration peak to appear after a lengthy induction period of 15–20 h, whereas the addition of seed in the absence of the activator has little effect. With presence of the activator, the addition of 1% seed causes a dramatic reduction in the induction period and increases the height of the hydration peaks. Fig. 2 shows the effects of varying the amount of C–S–H seed at a fixed activator concentration of 10%. For

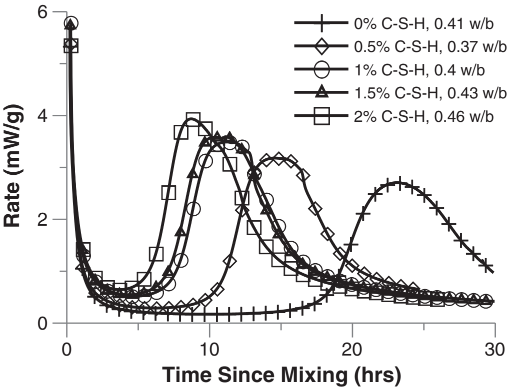

Fig. 2. Rate of heat evolution at 20 °C of slag pastes activated with 10% sodium metasilicate and made with varying amounts of C–S–H seed. The w/b was increased with the amount of seed to maintain workability.

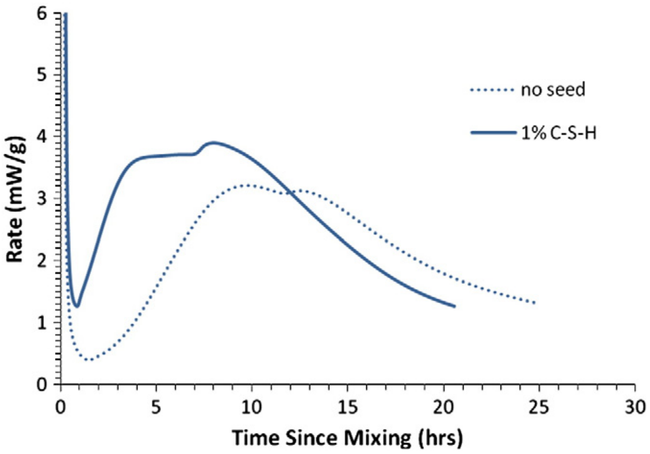

Fig. 3. Rate of heat evolution at 20 °C of OPC pastes with w/b = 0.40 made with and without C–S–H seed.

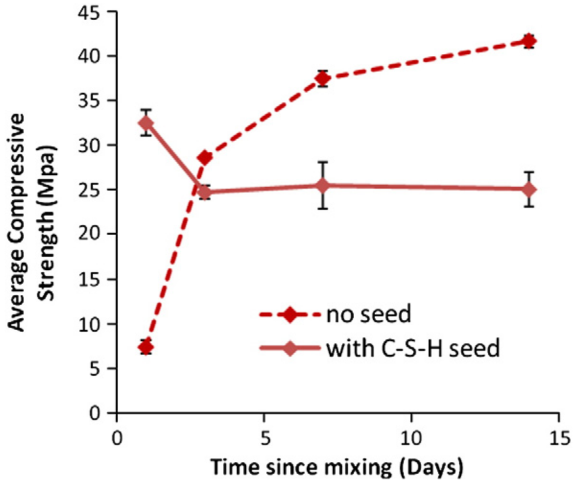

Fig. 5. Compressive strength development of AAS paste made with or without 1.33% C–S–H seed and cured with exposure to water. Pastes were exposed to 100% humidity for 1 d, then demolded and cured under lime water until the time of testing. All specimens were made with 10% sodium metasilicate activator and w/b = 0.43. Error bars show the standard deviation of three replicates.

these experiments, the w/b was increased as the amount of seed was increased to ensure a mixable paste. The w/b itself has little effect on the hydration kinetics. The general trend is that the hydration rate peaks are higher and occur earlier with more seed.

Fig. 3 shows the effect of 1% seed addition on OPC paste. As was observed previously for OPC paste [16], the rate peak becomes higher and is shifted earlier in time. The effect of seed is less dramatic than for AAS paste, however.

3.2. Compressive strength

The compressive strength development of AAS paste made with and without C–S–H seed (1.33% addition) and cured under sealed conditions is shown in Fig. 4. The strength development of identical AAS pastes cured under lime water is given in Fig. 5. As shown in Fig. 4, addition of 1 wt.% seed significantly increases the compressive strength under sealed conditions. After 24 h, the compressive strength of the seeded paste is ~5 times greater than that of the unseeded paste. As hydration continues out to 28 d, both pastes gain additional strength at about the same rate, such that the difference in compressive strength is approximately 14 MPa at all ages tested.

As shown in Fig. 5, with underwater curing very different strength development results are obtained for AAS with and without seed. For unseeded AAS paste, the compressive strength is higher at all ages as compared to sealed curing, and the 14 d strength is nearly twice as high (41.6 ± 0.7) MPa vs. (25.1 ± 1.9) MPa. In particular, the strength development of unseeded AAS is much greater between 1 d and 7 d with underwater curing than with sealed curing. This strongly suggests that the sealed pastes underwent self-desiccation that slowed the hydration process, as discussed in the next section.

Also shown in Fig. 5, the seeded pastes cured underwater developed a very high strength after 1 d (32.5 ± 1.5) MPa, but the strength then decreased to (24.7 ± 0.8) MPa at 3 d and remained at about that level thereafter. It should be noted that during the first 24 h of curing these pastes were not underwater but their upper surface was exposed to 100% RH air. The strength retrogression of the seeded AAS specimens cured underwater can be attributed to the development of visible crack lines along their outer surface, along which they later broke during compression testing.

The strength development of OPC pastes made with and without C–S–H seed (1% addition) and cured underwater conditions is shown in Fig. 6. In this case, the addition of seed increases the strength up to 3 d, but the strengths of seeded and unseeded OPC pastes at later ages (7–28 d) are similar. There was no evidence of cracking in any of the OPC specimens.

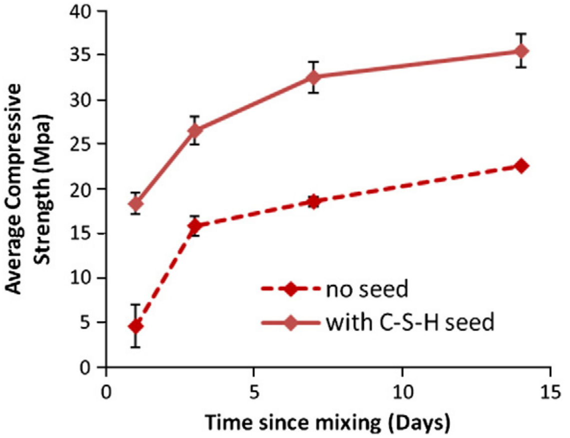

Fig. 4. Compressive strength development of AAS paste made with or without 1.33% C–S–H seed and cured under sealed conditions until the time of testing. All specimens were made with 10% sodium metasilicate activator and w/b = 0.43. Error bars show the standard deviation of three replicates.

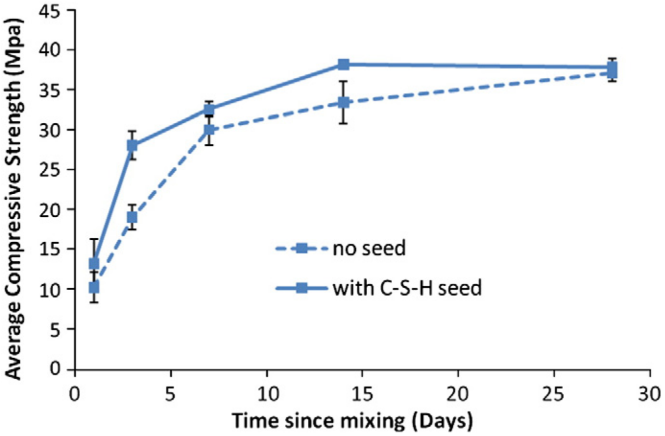

Fig. 6. Compressive strength development of OPC paste made with or without 1% C–S–H seed and cured with exposure to water. Pastes were exposed to 100% humidity for 1 d, then demolded and cured under lime water until the time of testing. All specimens were made with w/b = 0.42. Error bars show the standard deviation of three replicates.

4. Discussion

For OPC and C_3S pastes, it is well established that hydration at early times occurs by a nucleation and growth process that generates the characteristic main hydration rate peak (see recent reviews [18,19]). When activated with sodium metasilicate, the hydration of slag exhibits a similar hydration rate peak, suggesting that nucleation and growth is also rate controlling in this case. This is confirmed by the accelerating effect of C–S–H seed (see Fig. 1), since the seed would not otherwise be expected to have any effect. In the absence of alkali activation, the slag paste hydrates very slowly and does not respond to the addition of C–S–H seed, indicating that the rate at which the slag dissolves controls the hydration rate.

An interesting characteristic of the AAS hydration kinetics is the presence of a long induction period prior to the main hydration peak, which indicates that the initial nucleation process is slowed or delayed. Addition of nuclei in the form of C–S–H seed significantly shortens this initial dormant period. In OPC and C_3S pastes, nucleation occurs preferentially on the surface of the grains, and hydration product then grows outward from the grains into the capillary pore space [20–22]. It is not presently clear whether nucleation occurs directly on the surface of the grains or within a thin metastable product layer around the particles [18]. The long induction period exhibited by AAS pastes, combined with the observation [23] that early hydration product forms in the capillary space away from the grain surfaces, indicates that this heterogeneous surface nucleation process is not available for AAS paste.

The present results indicate that both the curing conditions (sealed or underwater) and the presence of C–S–H seed have important effects on the compressive strength development of AAS paste. The addition of C–S–H seed significantly increases the strength after 1 d of curing. This can be attributed to the fact that the seeded pastes have completely finished the main hydration peak after 1 d and are thus significantly more hydrated.

Trends in the compressive strength at later ages (after 1 d) are more complicated, but can be explained by the effects of autogenous shrinkage and cracking associated with chemical shrinkage. Chemical shrinkage is the decreased volume of the hydration products with respect to the reactants from which they form. Since the bulk volume of the paste cannot change significantly after initial set, chemical shrinkage causes emptying of internal pores. If the specimen can take up water from its surroundings, the pores will remain full and chemical shrinkage will have little effect. If not, the pores will begin to empty, starting with the largest. This will have two significant effects. First, the specimen will undergo shrinkage resulting from capillary stresses. Second, the hydration rate will decrease due to lack of availability of water for the hydration reactions.

Comparison of Figs. 4 and 5 shows that in the absence of C–S–H seed the strength development of AAS paste is much lower with sealed curing than with underwater curing. This indicates that even at very early ages the sealed paste undergoes autogenous shrinkage effects (slowed hydration, microcracking, or both) that are not experienced by the paste cured underwater. Previously it has been suggested or reported that the degree of chemical shrinkage of AAS paste is significantly greater than for OPC pastes [15,24], but recent calculations based on accurate measurements of the density and composition of the C–S–H formed in AAS paste indicate that the chemical shrinkage is similar to that of OPC paste [25]. However, the effects of autogenous shrinkage will depend not only on the amount of chemical shrinkage, but also on the pore structure of the products that form. Emptying of mesopores will have a much more significant effect on the hydration rate and internal stress development than emptying of capillary pores. There is considerable evidence that AAS hydration produces a much finer pore size distribution than OPC paste, with many nanometer-scale mesopores and fewer capillary pores [9,12], and this has been directly linked to the greater drying shrinkage exhibited by AAS pastes.

When AAS paste is made with C–S–H seed and exposed to 100% RH for 1 d, the strength is very high (see Fig. 5). However, following subsequent underwater curing the strength decreases and the specimens exhibit visible cracking on their outer surface. This can be attributed to the formation of a stress gradient in the sample. To completely relieve the internal stresses arising from pore emptying, water must be able to diffuse from the surface of the specimen to the interior at a rate sufficient to offset the chemical shrinkage arising from hydration. This will depend on the hydration rate, the permeability, and the minimum dimension of the specimen. We hypothesize that the rapid early hydration rate of AAS with C–S–H seed, combined with a rapid decrease in permeability arising from filling of the pore space with mesoporous hydration product, resulted in insufficiently rapid diffusion of water to the interior of these 2 in diameter specimens. Thus a stress gradient developed, with greater stress in the interior of the sample. Such a stress state is much more likely to cause cracking than the uniform stress state that forms during sealed curing.

For OPC hydrated underwater, there was no evidence of cracking from self-desiccation and the strength development after a few days of hydration was similar in the seeded and unseeded pastes (Fig. 6). It is well established that, in contrast to AAS, OPC hydration tends to occur primarily from the surface of the grains [23], leaving capillary diffusion paths. However, addition of C–S–H seed causes the capillary pore space to fill more completely [16], which could potentially lead to differential stresses and cracking during underwater curing. For the experiments conducted here, it appears that this was not the case.

The present results suggest that if the problems with self-desiccation could be avoided then the addition of C–S–H seed might result in significant increases in the long term strength of AAS paste. Future research along these lines would be useful. For example, other alkaline activators such as NaOH do not result in as much shrinkage as sodium silicate [2], and shrinkage-reducing admixtures are known to be effective for AAS [17].

5. Conclusions

The addition of C–S–H seed to AAS paste causes an earlier and larger hydration rate peak and a much higher compressive strength after 1 d of curing. The accelerating effect of seeding provides direct evidence that the early hydration process of AAS occurs by a nucleation and growth mechanism, as with Portland cement. The effect of C–S–H seed on the strength development of AAS after the first day of curing depended strongly on the curing method. With sealed curing, the strength continued to increase between 1 d and 14 d. For curing underwater, the strength decreased due to cracking. This cracking is attributed to differential stresses arising from chemical shrinkage. With underwater curing, water can flow into the sample, relieving the capillary stresses arising from chemical shrinkage. However, for the mix design and specimen size used here, water could only penetrate the surface region of the seeded AAS paste specimens, causing a stress gradient to form between the interior and exterior, leading to cracking. Because seeding shows strong potential for increasing both the early strength development and the long-term strength of AAS paste, further work aimed at controlling the internal stress state should be performed.

Acknowledgment

The authors would like to thank Nicholas Kappler for his assistance in performing the mixing and compressive strength measurements.

References

[1] G. Frigione, Manufacture and characteristics of Portland blast furnace slag cements, in: G. Frohndsdorff (Ed.), Blended Cements ASTM STP 897, American Society for Testing and Materials, Philadelphia, 1986, pp. 15–28.

[2] S.-D. Wang, X.C. Pu, K.S. Scrivener, P.L. Pratt, Alkali-activated slag cement and concrete: a review of properties and problems, Adv. Cem. Res. 7 (1995) 93–102.

[3] B. Lothenbach, K.L. Scrivener, R.D. Hooton, Supplementary cementitious materials, Cem. Concr. Res. 41 (2011) 217–229.

[4] S. Song, H.M. Jennings, Pore solution chemistry of alkali-activated ground granulated blast-furnace slag, Cem. Concr. Res. 29 (1999) 159–170.

[5] C. Shi, P.V. Krivenko, D.M. Roy, Alkali Activated Cements and Concretes, Taylor and Francis, New York (USA), 2006.

[6] E. Douglas, A. Bilodeau, J. Brandstetr, V.M. Malhotra, Alkali activated ground granulated blast-furnace slag concrete: preliminary investigation, Cem. Concr. Res. 21 (1991) 101–108.

[7] F. Bellmann, J. Stark, Activation of blast furnace slag by a new method, Cem. Concr. Res. 39 (2009) 644–650.

[8] F. Collins, J.G. Sanjayan, Cracking tendency of alkali activated slag subjected to restrained shrinkage, Cem. Concr. Res. 30 (2000) 791–798.

[9] T. Hakkinen, The influence of slag content on the microstructure, permeability, and mechanical properties of concrete. Part 1. Microstructural studies and basic mechanical properties, Cem. Concr. Res. 23 (1993) 407–421.

[10] M.B. Haha, G.L. Saout, F. Winnefeld, B. Lothenbach, Influence of activator type on hydration kinetics, hydrate assemblage and microstructural development of alkali activated blast-furnace slags, Cem. Concr. Res. 41 (2011) 301–310.

[11] S. Kourounis, S. Tsivilis, P.E. Tsakiridis, G.D. Papadimitrious, Z. Tsibouki, Properties and hydration of blended cements with steelmaking slag, Cem. Concr. Res. 37 (2007) 815–822.

[12] F. Collins, J.G. Sanjayan, Effect of pore size distribution on drying shrinkage of alkali-activated slag concrete, Cem. Concr. Res. 30 (2000) 1401–1406.

[13] A.A. Melo Neto, M.A. Cincotto, W. Repette, Drying and autogenous shrinkage of pastes and mortars with activated slag cement, Cem. Concr. Res. 38 (2008) 565–574.

[14] C.D. Atis, C. Bilim, O. Celik, O. Karahan, Influence of activator on the strength and drying shrinkage of alkali-activated slag mortar, Construction Building Materials 23 (2009) 548–555.

[15] W. Chen, H.J.H. Brouwers, The hydration of slag, Part 1: reaction models for alkali-activated slag, J. Mater. Sci. 42 (2007) 428–443.

[16] J.J. Thomas, H.M. Jennings, J.J. Chen, Influence of nucleation seeding on the hydration mechanisms of tricalcium silicate and cement, J. Phys. Chem. C 113 (2009) 4327–4334.

[17] M. Palacios, F. Puertas, Effect of shrinkage-reducing admixtures on the properties of alkali-activated slag mortars and pastes, Cem. Concr. Res. 37 (2007) 691–702.

[18] J.W. Bullard, H.M. Jennings, R.A. Livingston, A. Nonat, G.W. Scherer, J.S. Schweitzer, K.L. Scrivener, J.J. Thomas, Mechanisms of cement hydration at early ages, Cem. Concr. Res. (2011), doi:10.1016/j.cemconres.2010.09.011.

[19] J.J. Thomas, J.J. Biernacki, J.W. Bullard, S. Bishnoi, J.S. Dolado, G.W. Scherer, A. Luttge, Modeling and simulation of cement hydration kinetics and microstructure development, Cem. Concr. Res. (2011), doi:10.1016/j.cemconres.2010.10.004.

[20] J.J. Thomas, A new approach to modeling the nucleation and growth kinetics of tricalcium silicate hydration, J. Am. Ceram. Soc. 90 (2007) 3282–3288.

[21] S. Bishnoi, K.L. Scrivener, Studying nucleation and growth kinetics of alite hydration using μic, Cem. Concr. Res. 39 (2009) 849–860.

[22] J.J. Thomas, A.J. Allen, H.M. Jennings, Hydration kinetics and microstructure development of normal and $CaCl_2$-accelerated tricalcium silicate (C_3S) pastes, J. Phys. Chem. C 113 (2009) 19836–19844.

[23] A. Gruskovnjak, B. Lothenbach, L. Holzer, R. Figi, F. Winnefeld, Hydration of alkali-activated slag: comparison with ordinary Portland cement, Adv. Cem. Res. 18 (2006) 119–128.

[24] D.P. Bentz, Internal curing of high-performance blended cement mortars, ACI Mater. J. (July-August 2007) 408–414.

[25] J.J. Thomas, A.J. Allen, H.M. Jennings, Density and water content of solid nanoscale C–S–H formed in alkali-activated slag (AAS) paste and implications for chemical shrinkage (submitted for publication).